Chapter 3: Observations: Surface and Atmospheric Climate Change

Coordinating Lead Authors: Philip D. Jones, Kevin E. Trenberth

Lead Authors: Peter G. Ambenje, Roxana Bojariu, David R. Easterling, Albert M. G. Klein Tank, David E. Parker, James A. Renwick, Fatemeh Rahimzadeh, Matilde M. Rusticucci, Brian J. Soden, Pan-Mao Zhai

Contributing Authors: R. Adler, L. Alexander, H. Alexandersson, R. P. Allan, M. P. Baldwin, M. Beniston, D. H. Bromwich, I. Camilloni, C. Cassou, D. R. Cayan, E. K. M. Chang, J. R. Christy, A. Dai, C. Deser, N. Dotzek, R.L. Fogt, C. K. Folland, P. Forster, M. Free, C. Frei, B. Gleason, J. Grieser, P. Y. Groisman, S. K. Gulev, J. W. Hurrell, M. Ishii, S. A. Josey, P. W. Kållberg, G. N. Kiladis, R.H. Kripalani, K. E. Kunkel, C-Y. Lam, J. R. Lanzante, J. H. Lawrimore, D. H. Levinson, B. G. Liepert, G. J. Marshall, C. A. Mears, P. W. Mote, H. Nakamura, N. Nicholls, J. R. Norris, T. Oki, F. R. Robinson, K. Rosenlof, F. H. Semazzi, D. J. Shea, J. M. Shepherd, T. G. Shepherd, S. C. Sherwood, A. J. Simmons, I. Simmonds, P. C. Siegmund, C. D. Thorncroft, P. D. Thorne, S. M. Uppala, R. S. Vose, B. Wang, S. G. Warren, R. Washington, M. C. Wheeler, B. A. Wielicki, T. Wong.

Review Editors: Brian J. Hoskins, Bubu P. Jallow, Tom R. Karl

Date of Draft: 12 August 2005:

Notes: This is the TSU compiled version.

Figures

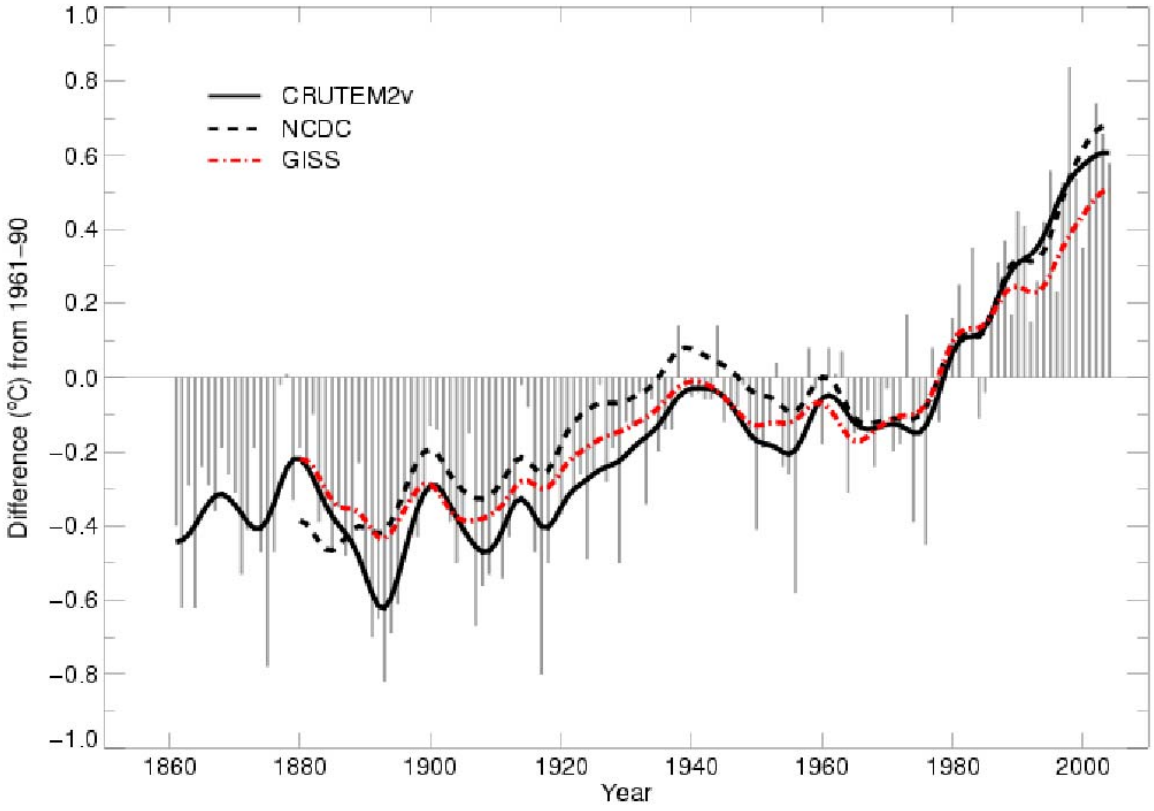

Figure 3.2.1. Annual anomalies of global land surface air temperature, 1861 to 2004, relative to 1961 to 1990 (°C) for CRUTEM2v updated from Jones and Moberg (2003). The smooth curves were created using a 21-point binomial filter to give near-decadal averages. The thick solid black curve from CRUTEM2v is compared with a corresponding smoothed curves based on the NCDC (Reynolds and Smith, 2005) series (dashed) and GISS (Hansen et al., 2001) (red dashed).

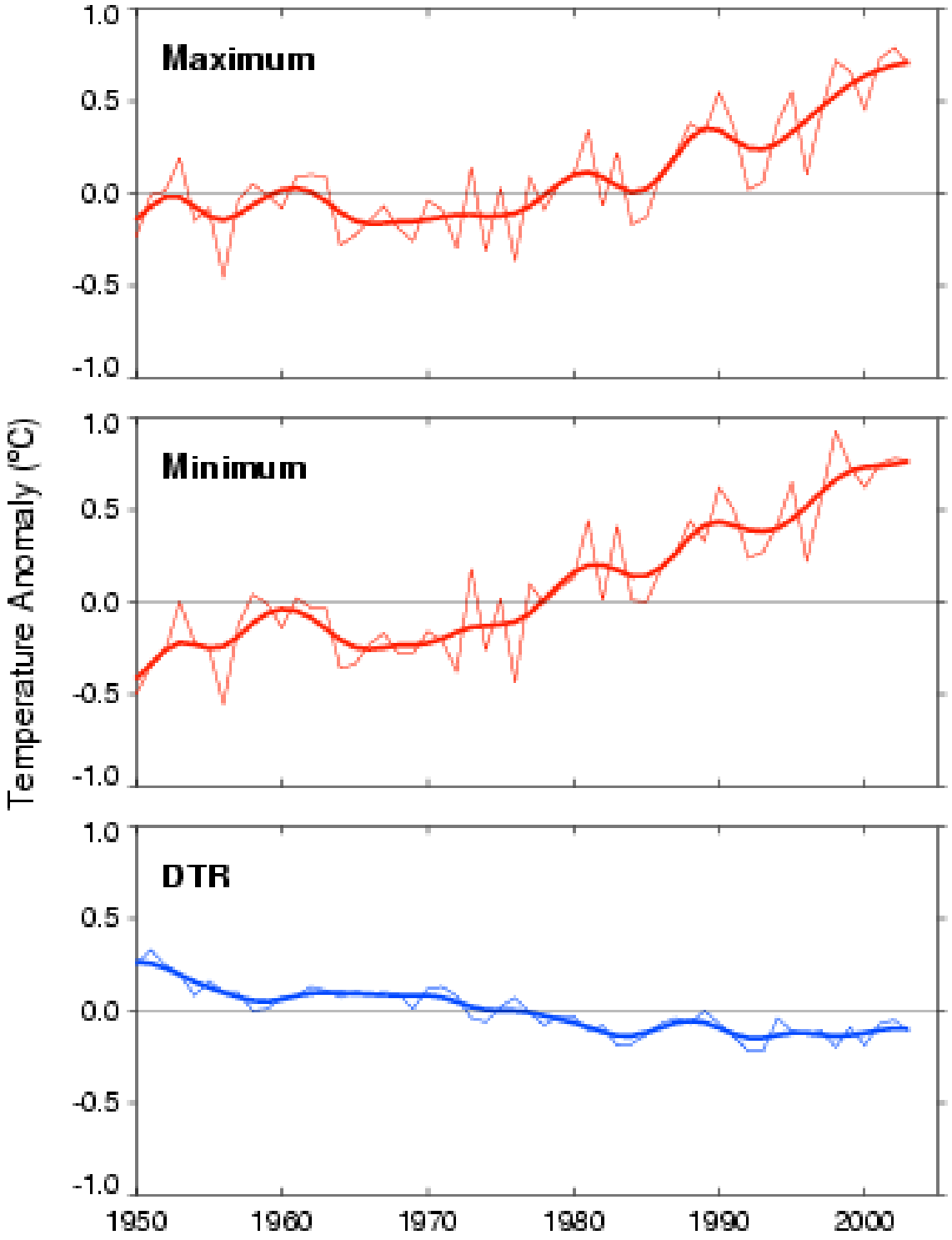

Figure 3.2.2. Annual values of maximum and minimum temperatures and diurnal temperature range averaged for the 71% of global land areas where data are available. The smoothed curve is from a 9 point binomial filter to show the decadal variability. From Vose et al. (2005).

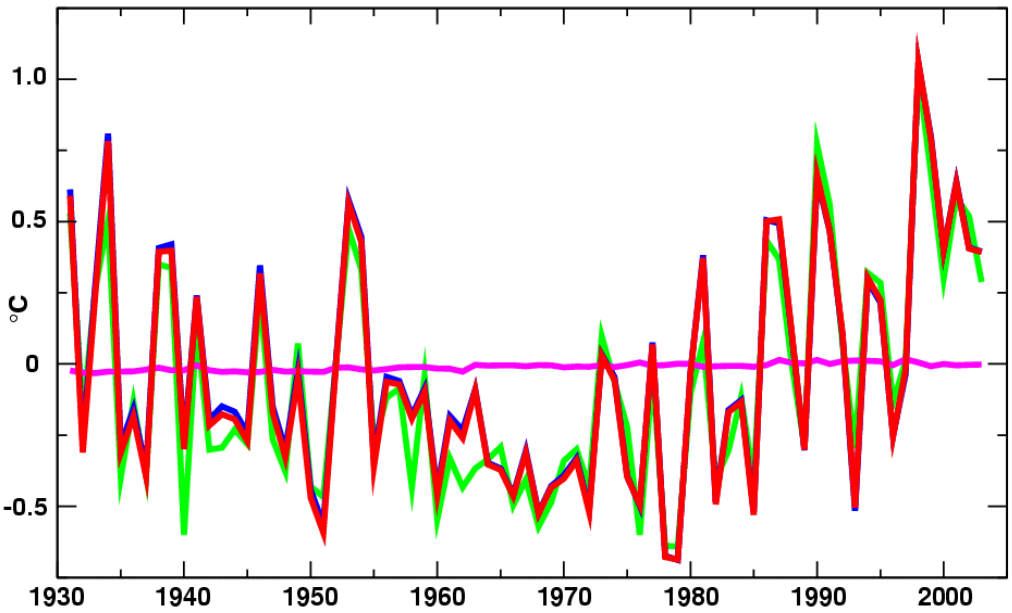

Figure 3.2.3. Anomaly time series of the full USHCN data (red), the USHCN data without the 16% of the stations with populations of over 30,000 within 6 km in the year 2000 (blue), and the 16% of the stations with populations over 30,000 (green). The full data set values minus the set without the most urban stations are shown in magenta. Both the full data set and the data set without the high population stations had stations in all of the 2.5° latitude by 3.5° longitude grid boxes during the entire period plotted but the subset of high population stations only had data in 56% of these grid boxes.

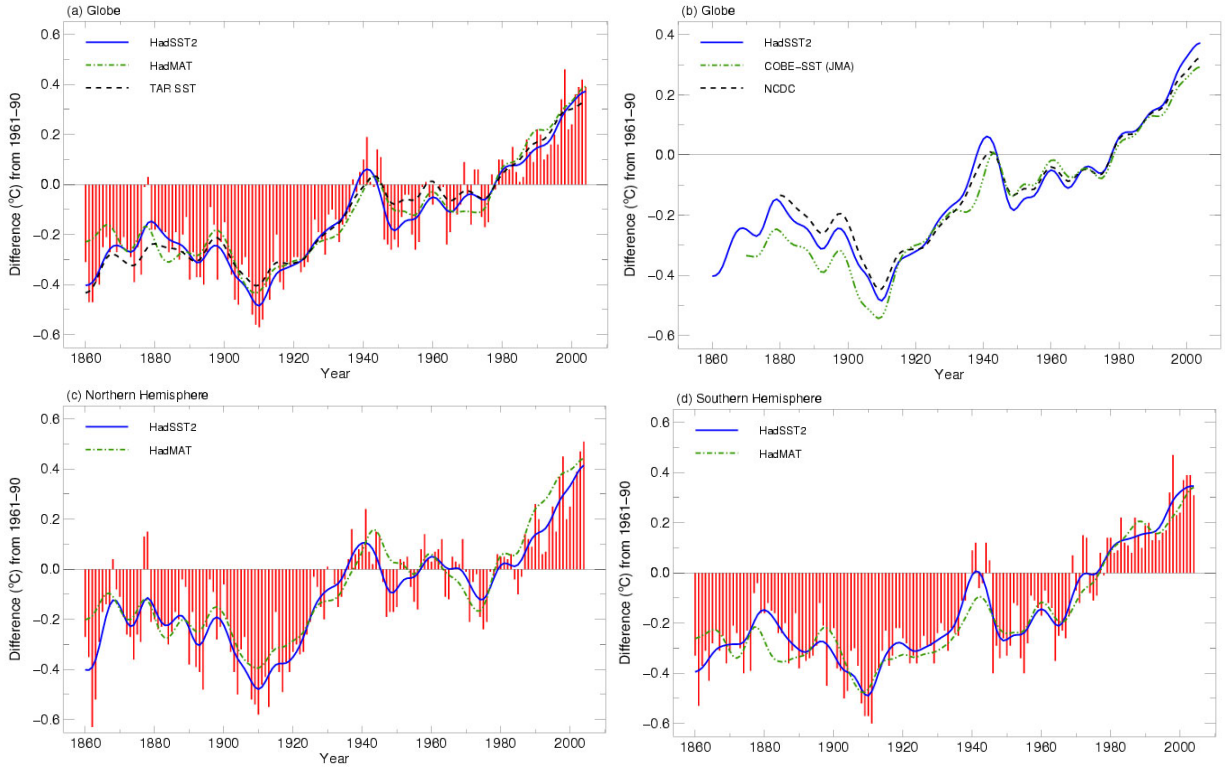

Figure 3.2.4. (a) Annual anomalies of global SST (HadSST2; red bars and blue solid curve) and global night marine air temperature (NMAT, dotted green curve), 1861 to 2004, relative to 1961 to 1990 (°C) from UKMO (Rayner et al., 2005). The smooth curves were created using a 21-point binomial filter to give near-decadal averages. The dashed black curve shows equivalent smoothed SST anomalies from the TAR. (b) Smoothed annual global SST 1861 to 2004, relative to 1961 to 1990 (°C), from UKMO (thick blue line as in a) and from Reynolds et al. (2002) (NCDC; dashed black line, includes satellite data) 1961 to 1990 (°C), and from Japan [(Ishii et al., 2005) COBE-SST (JMA)], green dashed line. (c, d) As in (a) but for the Northern and Southern Hemispheres and showing only the Rayner et al. (2005) series.

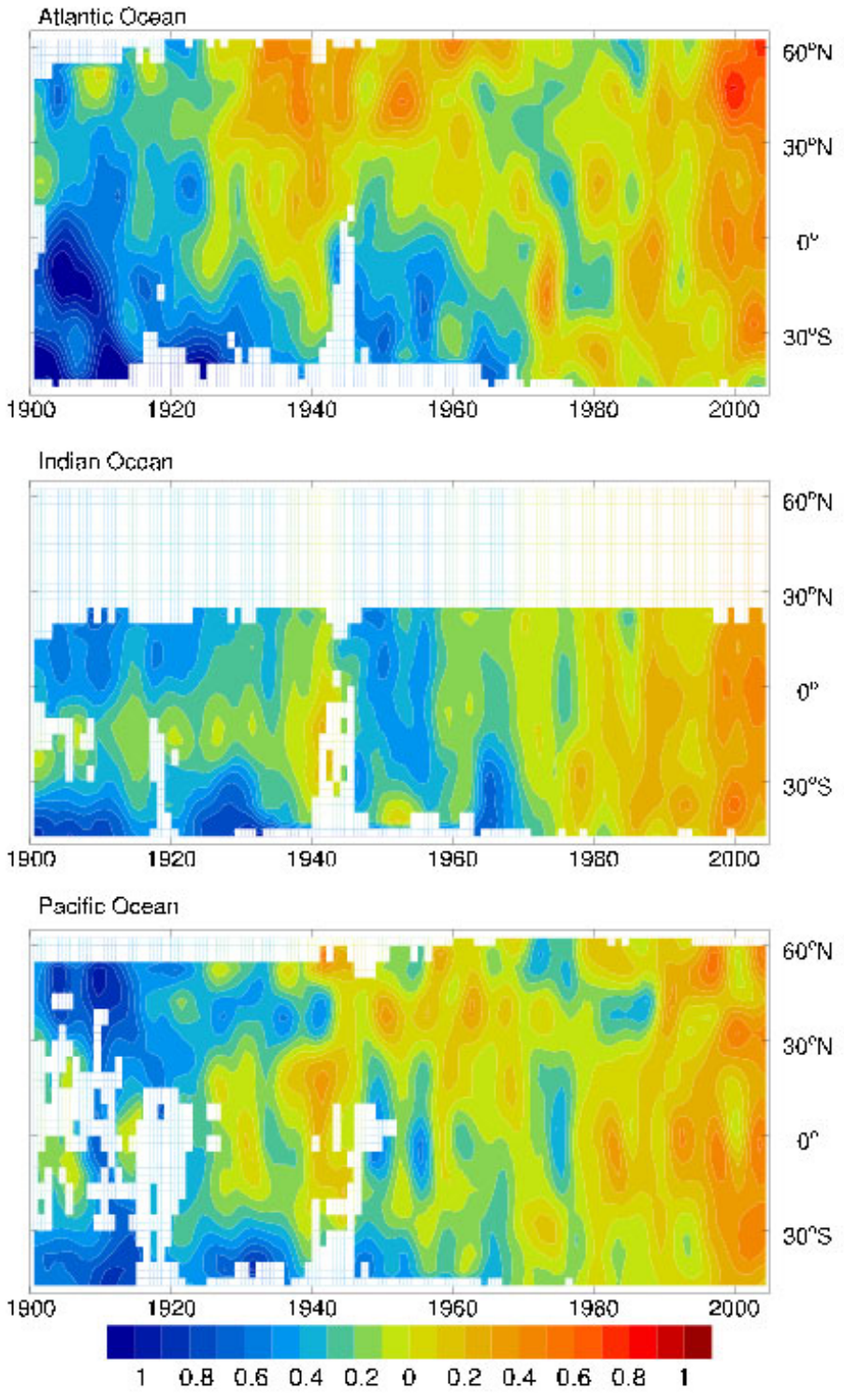

Figure 3.2.5. Latitude-time sections for the zonal mean across each ocean of annual anomalies of SST (°C) from 1900 to 2004 relative to 1961 to 1990 from UKMO (Rayner et al., 2005). The values are smoothed with a 1/12(1–3–4–3–1) filter to remove fluctuations less than 6 years or so, including the ENSO signal.

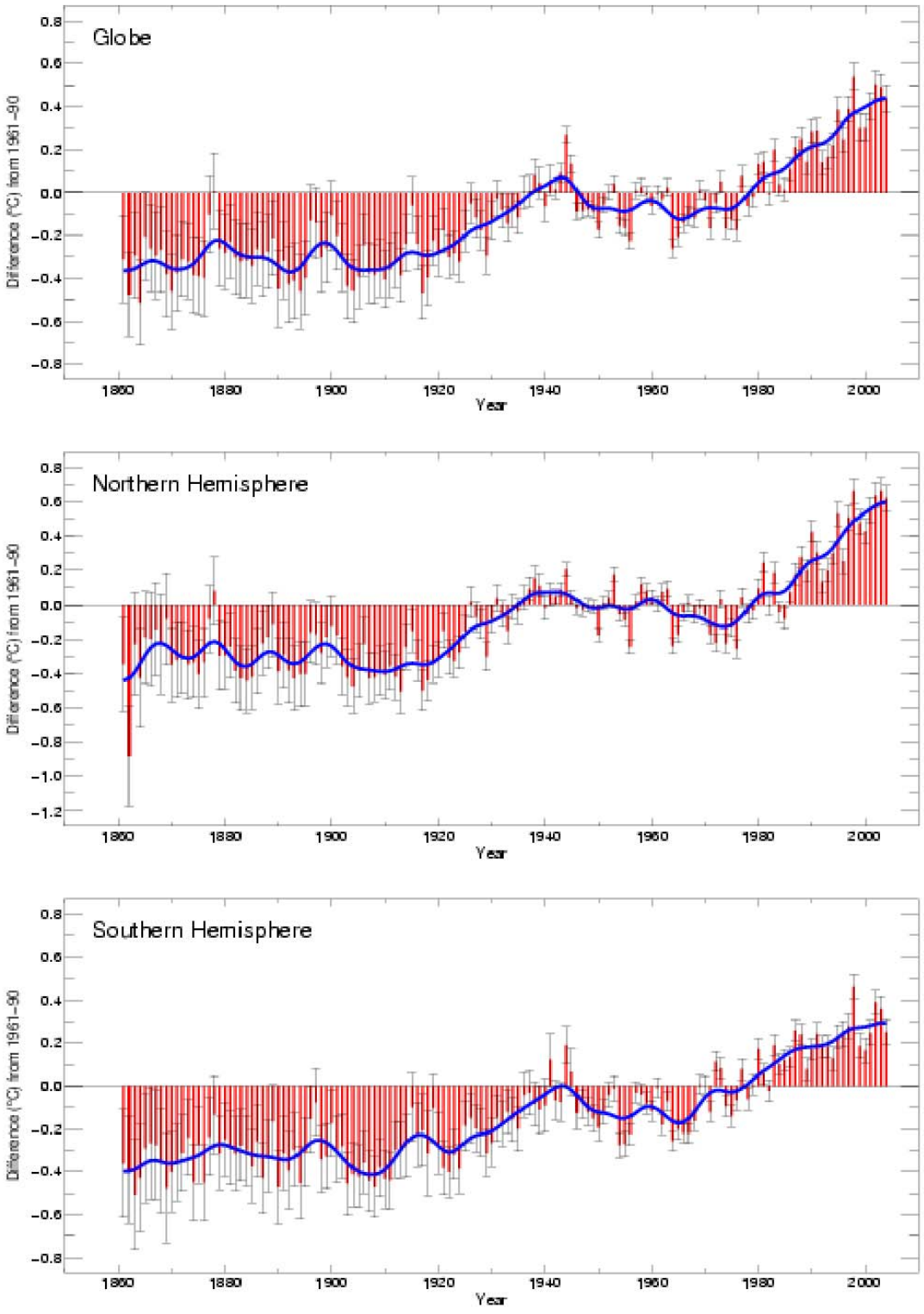

Figure 3.2.6. Global and hemispheric series of combined SST and land surface air temperature from the CRU-UKMO analysis (Parker et al., 2004). Annual error bars were estimated as in Folland et al. (2001) and the TAR. The smooth blue curves were created using a 21-point binomial filter giving near-decadal averages.

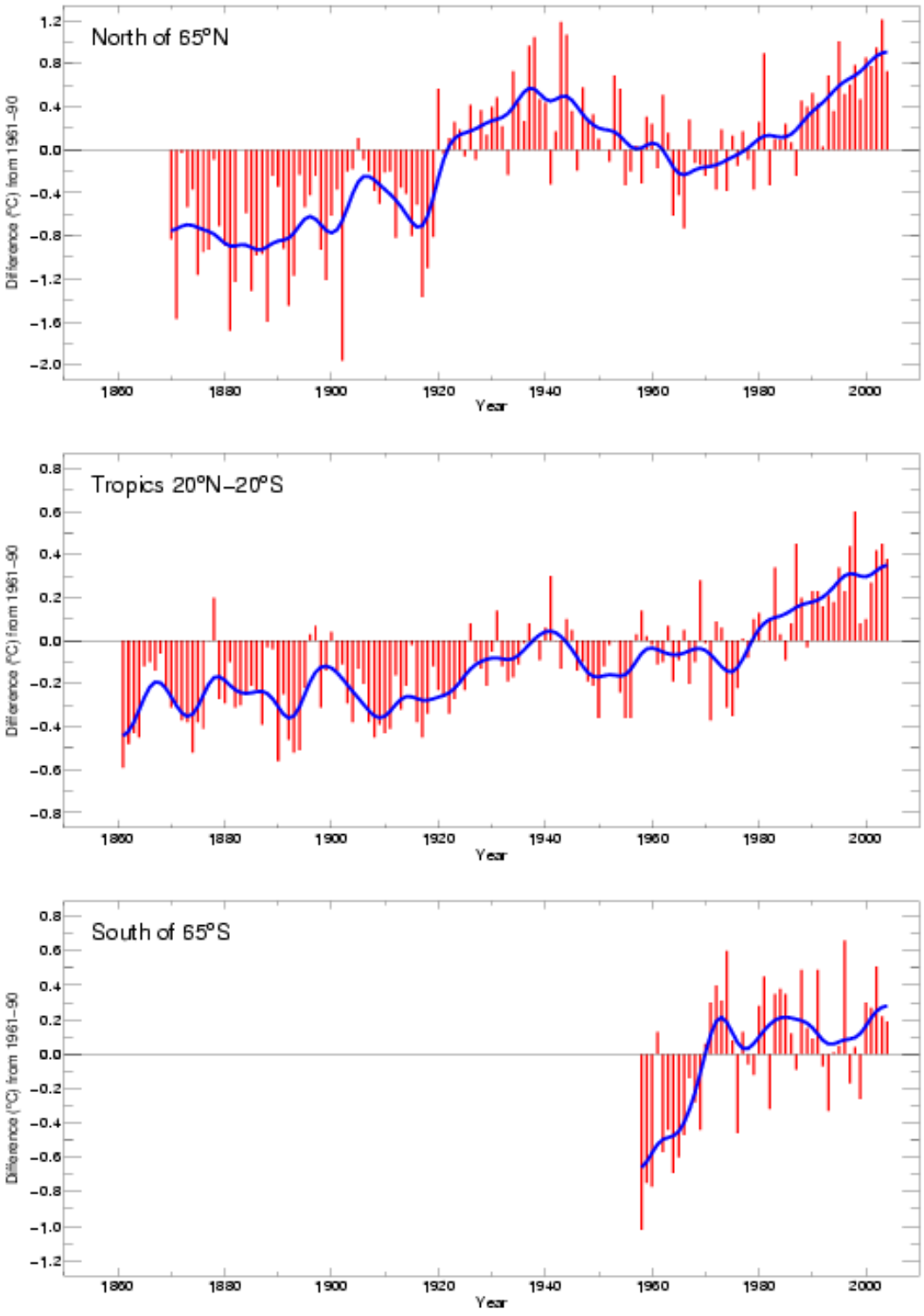

Figure 3.2.7. Time series of combined SST and land surface air temperature from the CRU-UKMO analysis (Parker et al., 2004) for the tropics (20°N–20°S), and for the polar regions north and south of 65°. The smooth curves were created using a 21-point binomial filter giving near-decadal averages.

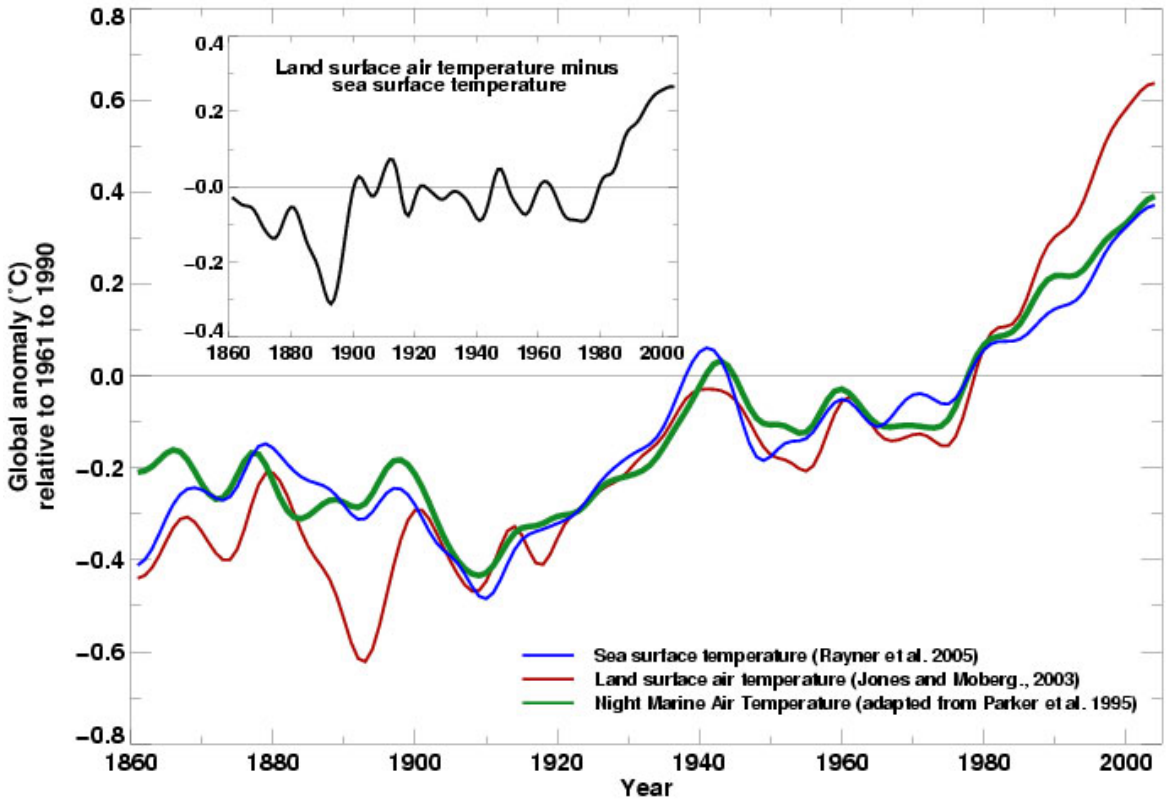

Figure 3.2.8. Smoothed annual anomalies of global average sea surface temperature (blue curve), night marine air temperature (green curve) and land surface air temperature (red curve) 1861 to 2004, relative to 1961 to 1990 (°C) (Rayner et al., 2005; Jones and Moberg, 2003). The smooth curves were created using a 21-point binomial filter to give near-decadal averages. Also shown (inset) are the smoothed differences between the land-surface air and sea surface temperature anomalies.

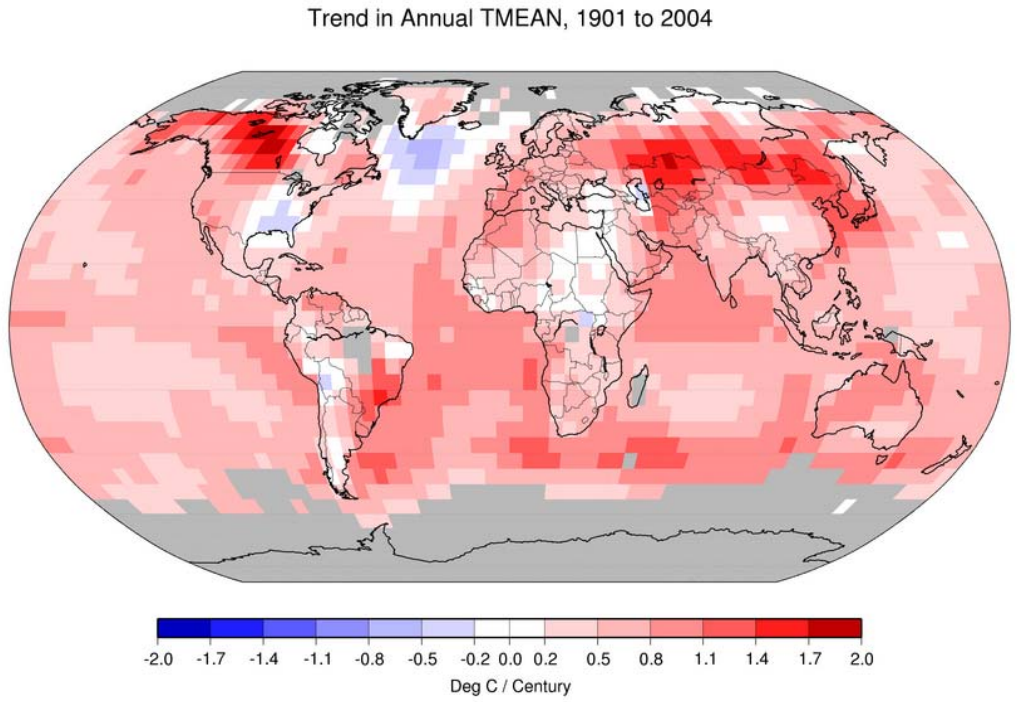

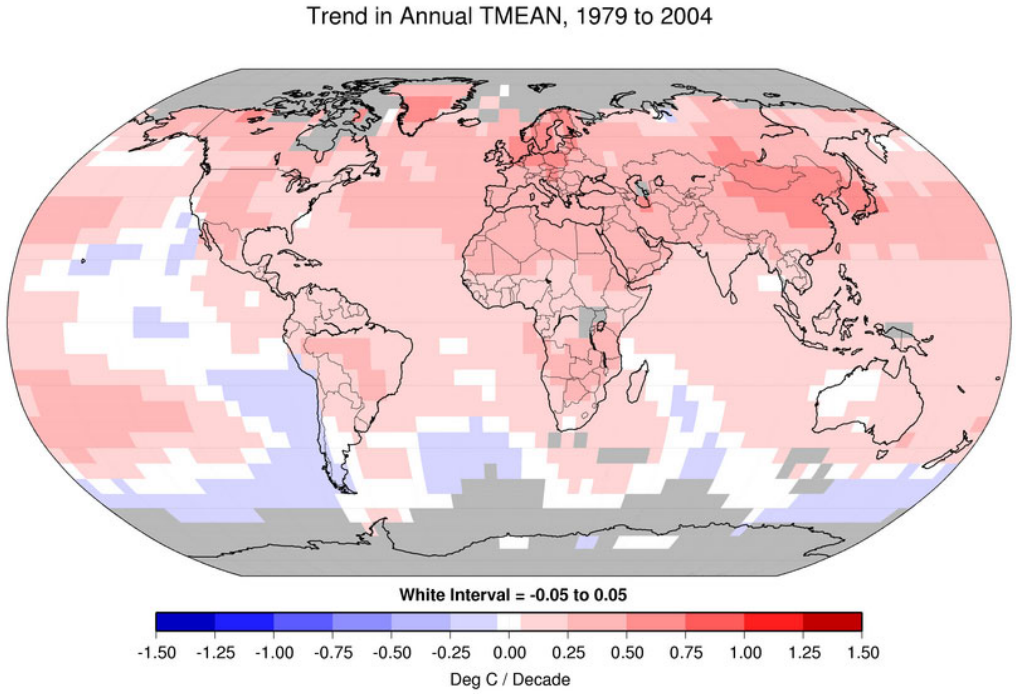

Figure 3.2.9. Linear trend of annual temperatures for 1901–2004 (upper) and 1979–2004 (lower). Areas in grey have incomplete data to produce reliable trends. The units are °C century^{-1}. The minimum number of years needed to calculate a trend value is 66 valid years during 1901–2004 period and 18 years for 1979–2004. An annual value is complete for a given year if there were 10 valid monthly temperature anomaly values. The dataset used was produced by NCDC from Smith and Reynolds (2005).

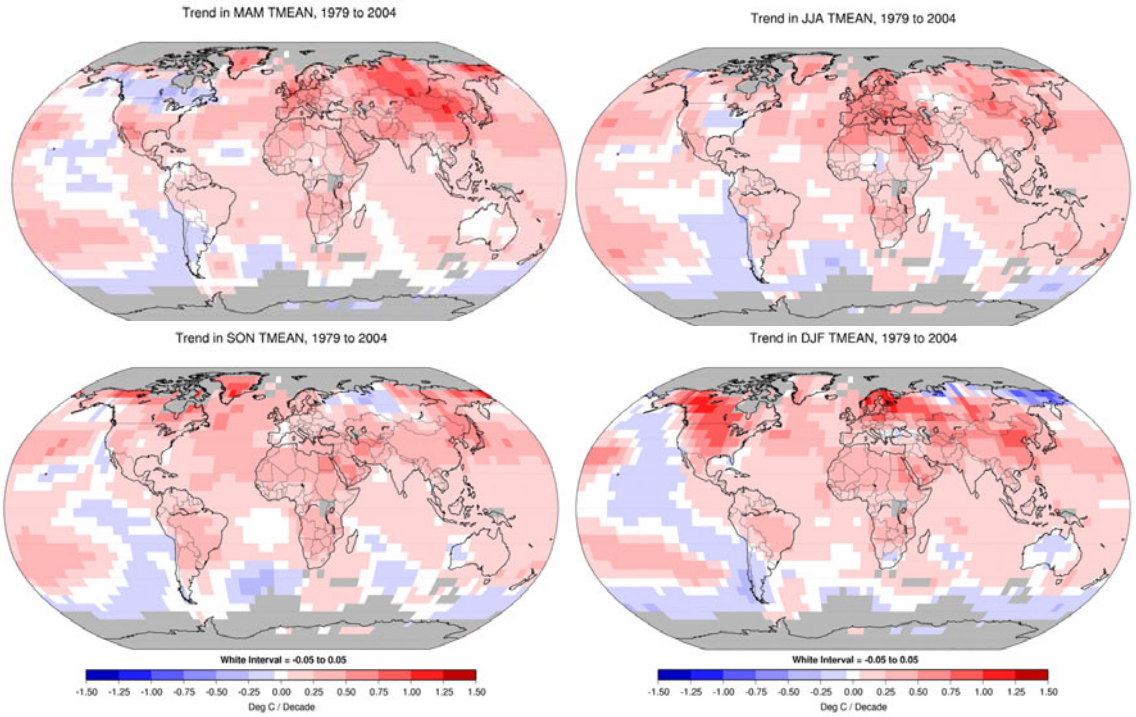

Figure 3.2.10. Linear trend of seasonal MAM, JJA, SON and DJF temperature trends for 1979–2004. Areas in grey have incomplete data to produce reliable trends. The units are °C decade^{-1}. The minimum number of years to calculate a trend value is 18 during 1979-2004. A seasonal value is complete for a given season if there were 2 valid monthly temperature anomaly values. The dataset used was produced by NCDC from Smith and Reynolds (2005).

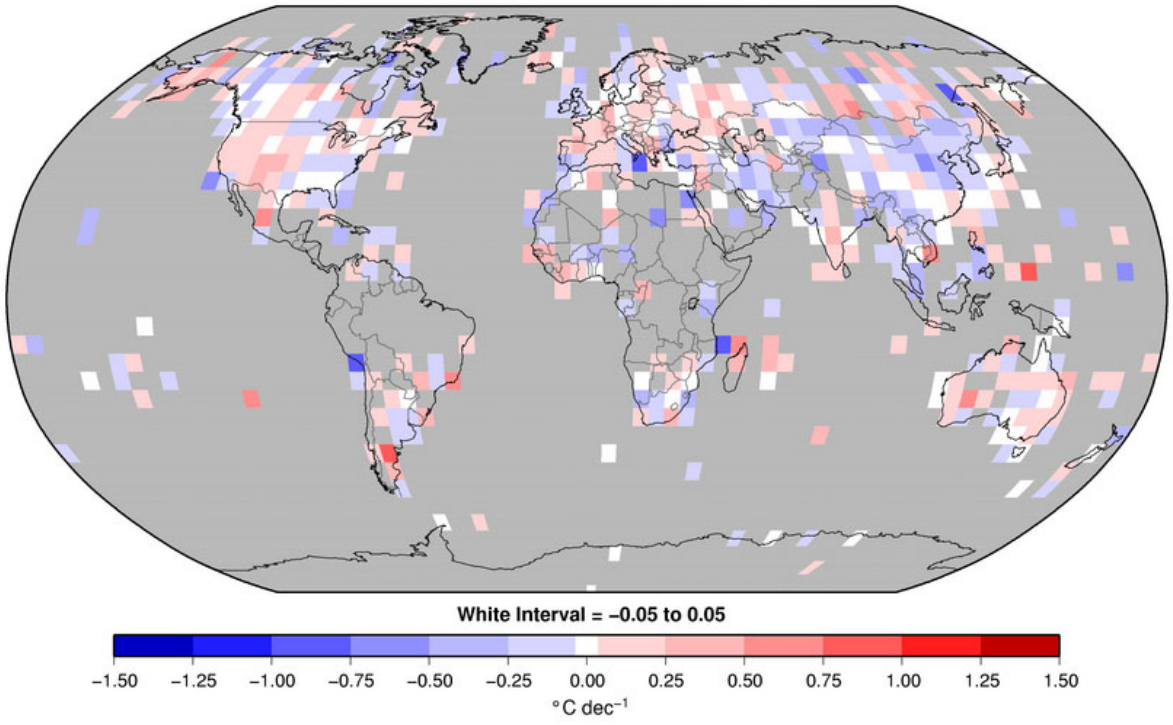

Figure 3.2.11. Linear trend in annual mean DTR for 1979 to 2004 in °C decade^{-1}. Grey regions indicate incomplete or missing data. After Vose et al. (2005).

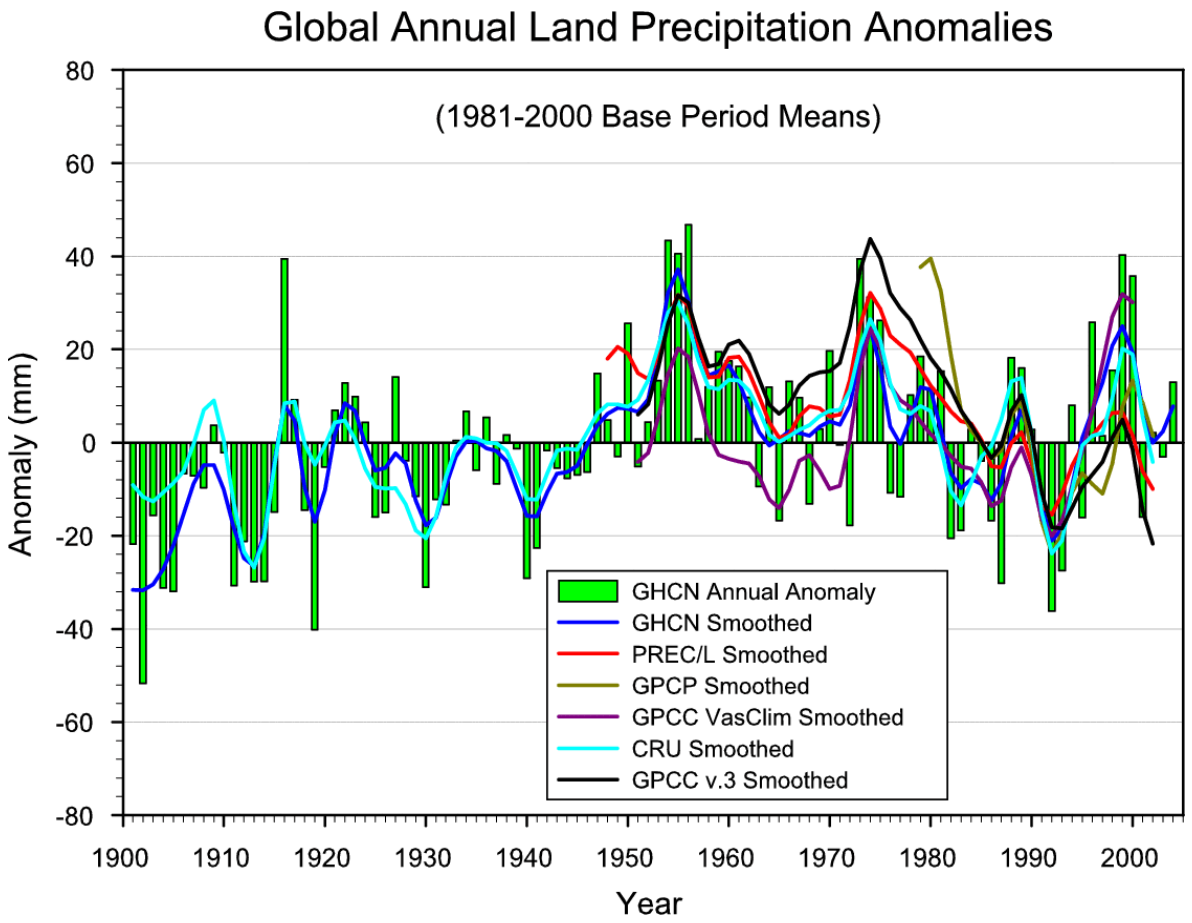

Figure 3.3.1. Time series of annual global land precipitation anomalies with respect to the 1961–1990 base period for 1900 to 2004 (to convert to mm/day divide by 365 or 366). Smoothed values (using the filter in Figure 3.2.5) are also given for the GHCN (Peterson and Vose, 1997), GPCC (Rudolf et al., 1994), CRU (New et al., 2001), Chen et al. (2002) and GPCP (Adler et al., 2003).

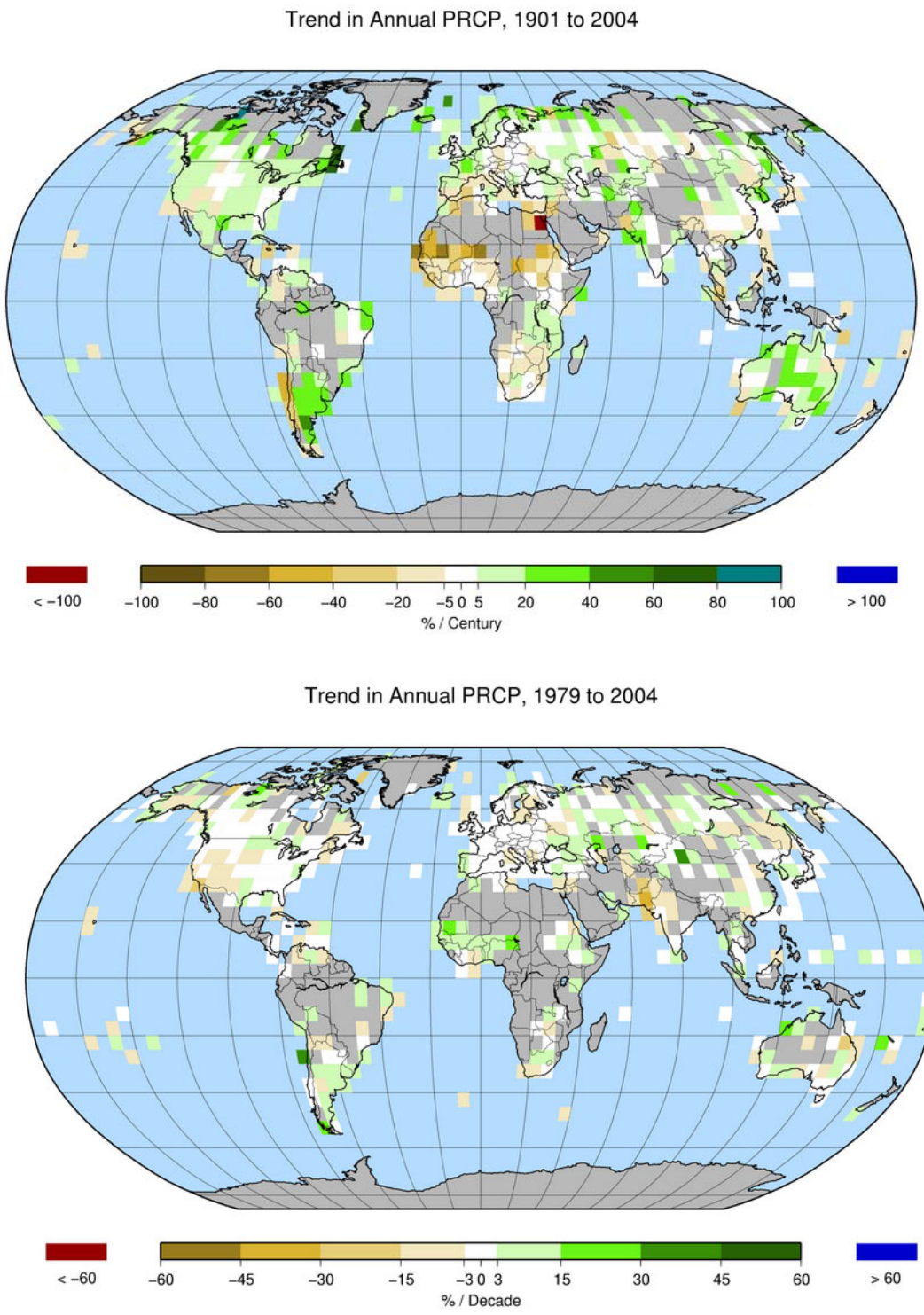

Figure 3.3.2. Trend of annual precipitation amounts for 1901–2004 (upper) and 1979–2004 (lower). Areas in grey have incomplete data to produce reliable trends. The units are % century^{-1}, the percentage being based on the 1961–1990 period. The minimum number of years to calculate a trend value is 66 valid years during 1901–2004 period and 18 years for 1979–2004. An annual value is complete for a given year if all twelve monthly percentage anomaly values were present. The GHCN precipitation dataset from NCDC was used.

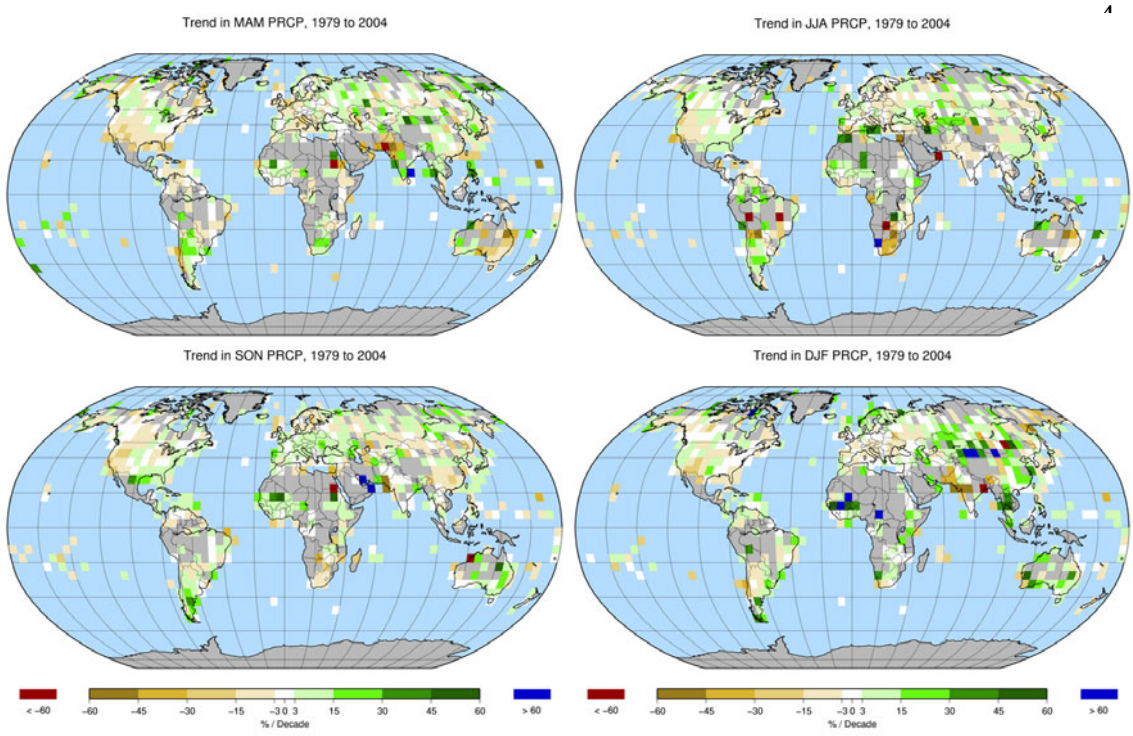

Figure 3.3.3. Trend of seasonal MAM, JJA, SON and DJF precipitation amounts for 1979–2004. Areas in grey have incomplete data to produce reliable trends. The units are % decade^{-1}, the percentage being based on the 1961–1990 period. The minimum number of years to calculate a trend value is 18 during 1979–2004. A seasonal value is complete for a given season if all three monthly anomaly values were present. The GHCN precipitation dataset from NCDC was used.

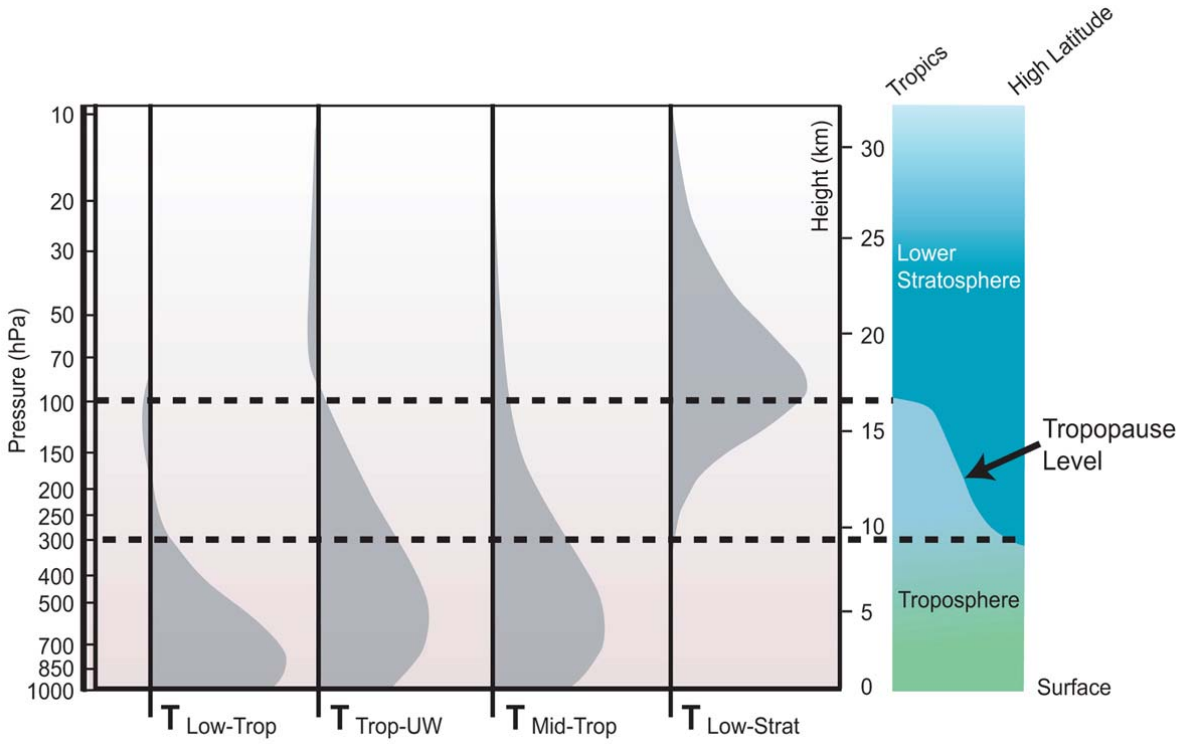

Figure 3.4.1. Vertical weighting functions depicting the layers sampled by satellite MSU measurements and their derivatives, and used also for radiosonde and reanalysis records. The right panel schematically depicts the variation in the tropopause from the tropics (left) to the high latitudes (right) and thus the dividing line between the stratosphere and troposphere. The fourth panel depicts T4 in the lower stratosphere, the third panel shows T2 (also called mid-troposphere), the second panel shows the troposphere as a combination of T2 and T4 (Trop-UW, Fu et al., 2004a), and the first panel shows $T2_{LT}$ from UAH for the low troposphere. Adapted from CCSP (2005) NRC review draft.

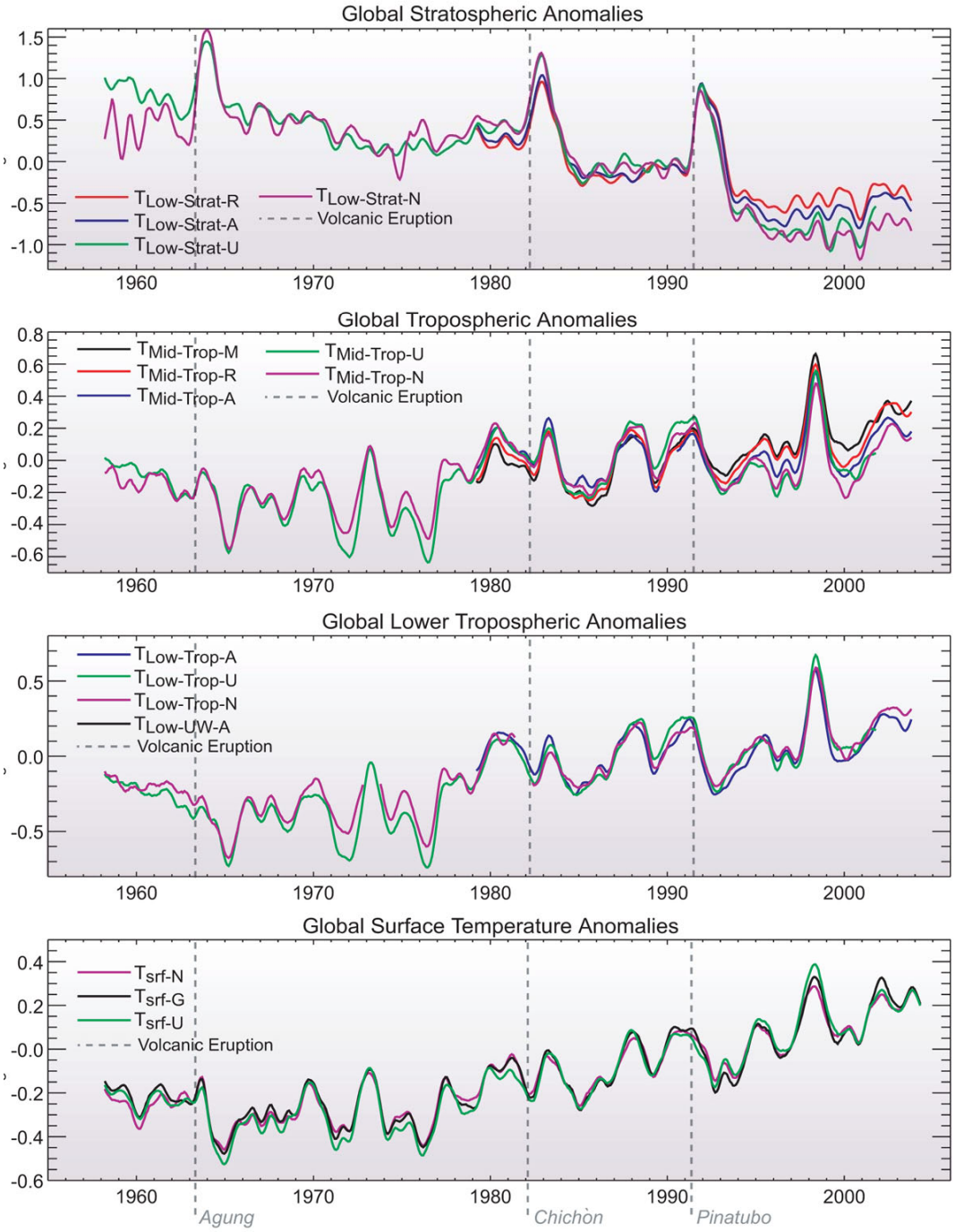

Figure 3.4.2. Observed surface and upper air temperatures. Bottom: surface records from NOAA (srf-N), NASA GISS (srf-G) and UKMO/CRU (srf-U). Lower middle: Lower tropospheric (Low-Trop) records from UAH (A) from MSU satellite observations, UKMO HadAT2 (U) and NOAA RATPAC (N) radiosonde observations. The modified tropospheric record from the University of Washington (Fu et al 2004a) (UW) is also shown based on UAH MSU. Upper middle: Tropospheric T2 records from UAH (A), RSS (R), UMD (M) (VG2) and equivalent radiosonde based values from HadAT2 (U) and RATPC (N). Top: Lower stratospheric (Low-Strat) T4 records. All time series are based on monthly mean anomalies relative to 1979 to 1997 smoothed with a 7 month running mean filter. Adapted from CCSP (2005) NRC review draft. To be updated through 2004 and with corrected $T2_{LT}$ from UAH and new RSS added.

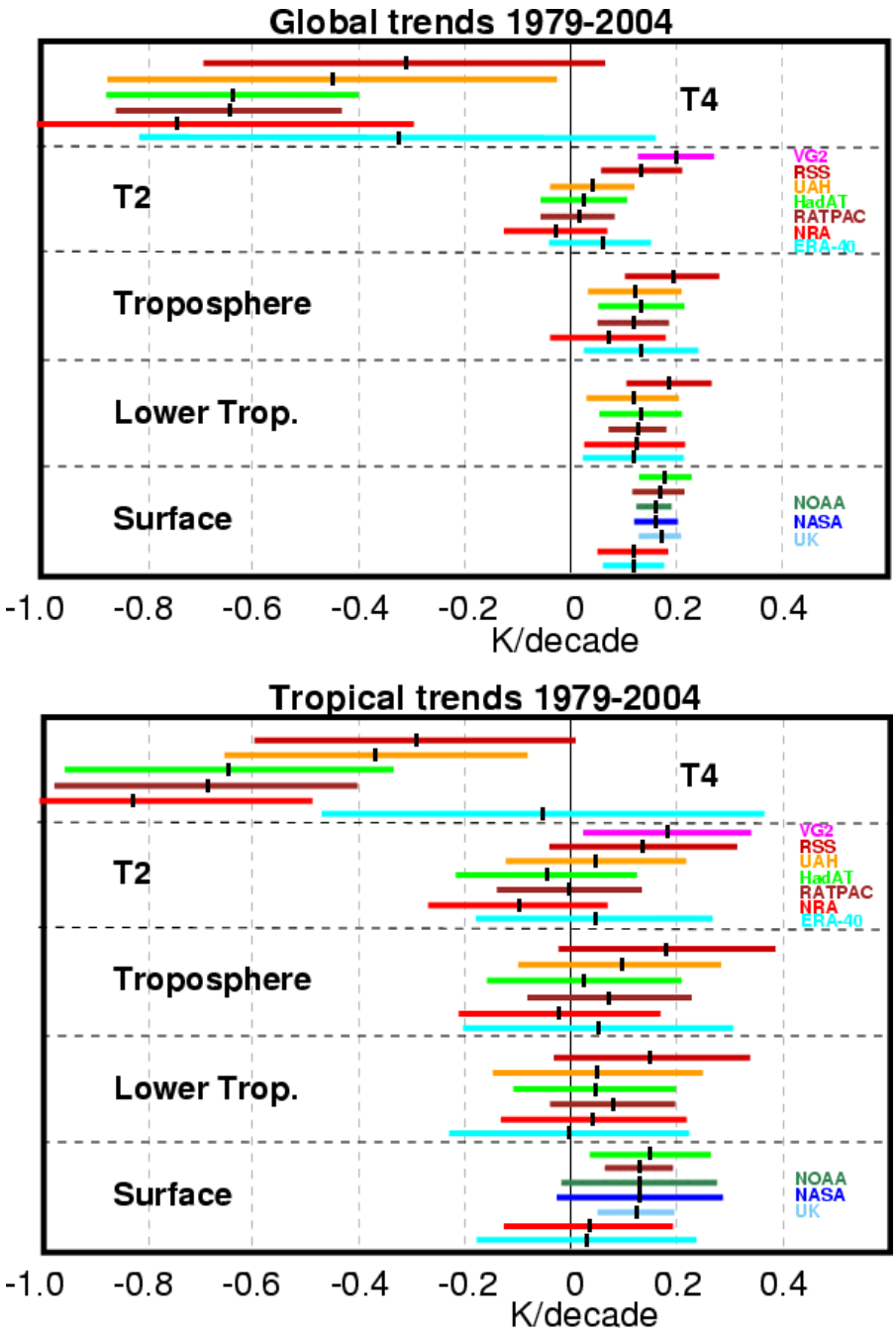

Figure 3.4.3. Linear trends (K decade^{-1}) for 1979–2004 for globe (top) and tropics 20ºN–20ºS (lower) for the MSU channels T4 (top panel) and T2 (second panel) or equivalent for radiosondes and reanalyses; for the troposphere (third panel) based on T2 with T4 used to statistically remove stratospheric influences (Fu et al., 2004a); the lower troposphere (fourth panel) based on the UAH retrieval profile; and the surface (bottom panel). Surface only records are from NOAA NCDC (green), NASA GISS (blue) and UKMO/CRU (light blue). Satellite records are from UAH (orange), RSS (dark red) and VG2 (pink); radiosonde based records are from NOAA RATPAC (brown), and HadAT2 (light green); and atmospheric reanalyses are from NCEP/NCAR (NRA red), and ERA-40 (cyan). Confidence limits are 95% (two standard errors) temporal sampling with an allowance for autocorrelation. Where the confidence limits exceed –1, the values are truncated. ERA-40 trends are only for 1979 to August 2002. Data from CCSP (2005, from D. Seidel, courtesy J. Lanzante), and J. Christy.

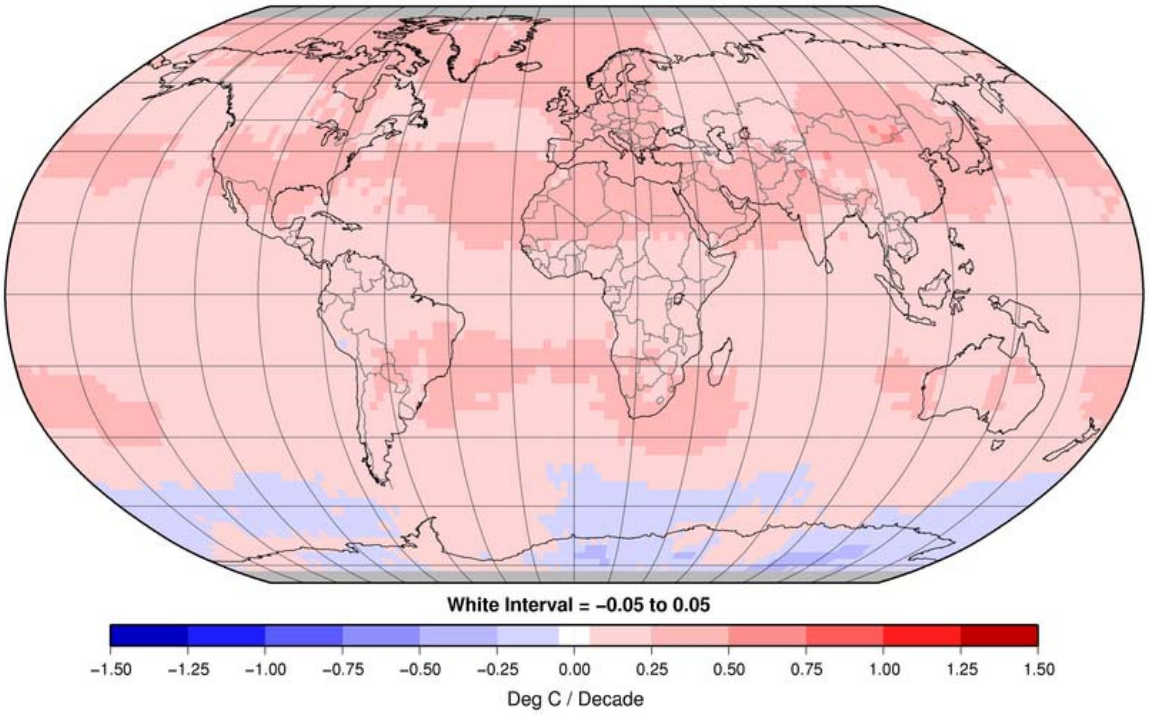

Figure 3.4.4. Linear trends for 1979–2004 for the troposphere from RSS (based on T2 and T4 adjusted as in Fu et al., 2004a) in K decade^{-1}. Courtesy Q. Fu.

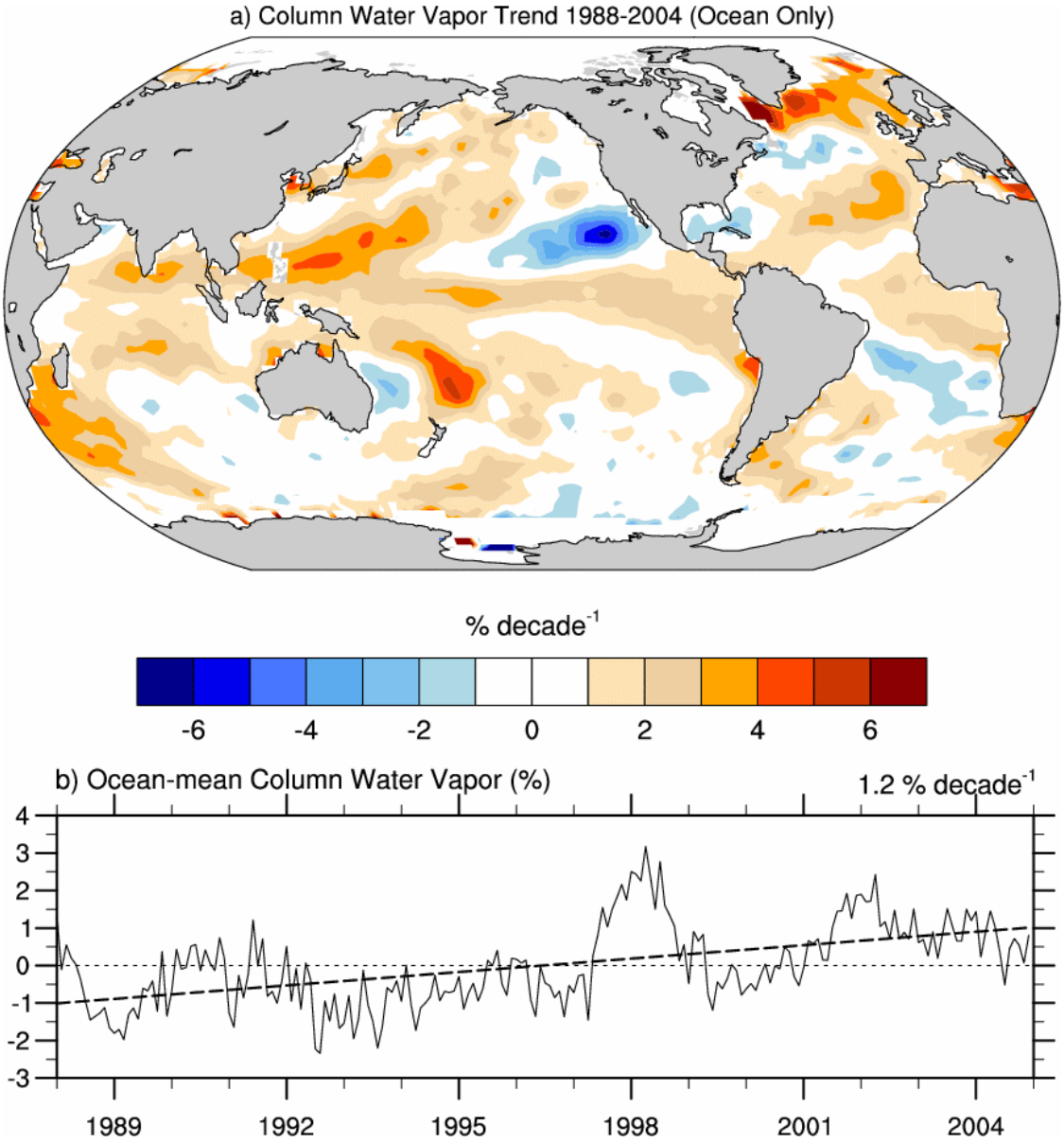

Figure 3.4.5. Linear trends in precipitable water for 1988–2004 in % per decade (top) and monthly time series of anomalies over the global ocean plus linear trend (bottom), from RSS SSM/I (updated from Trenberth et al., 2005).

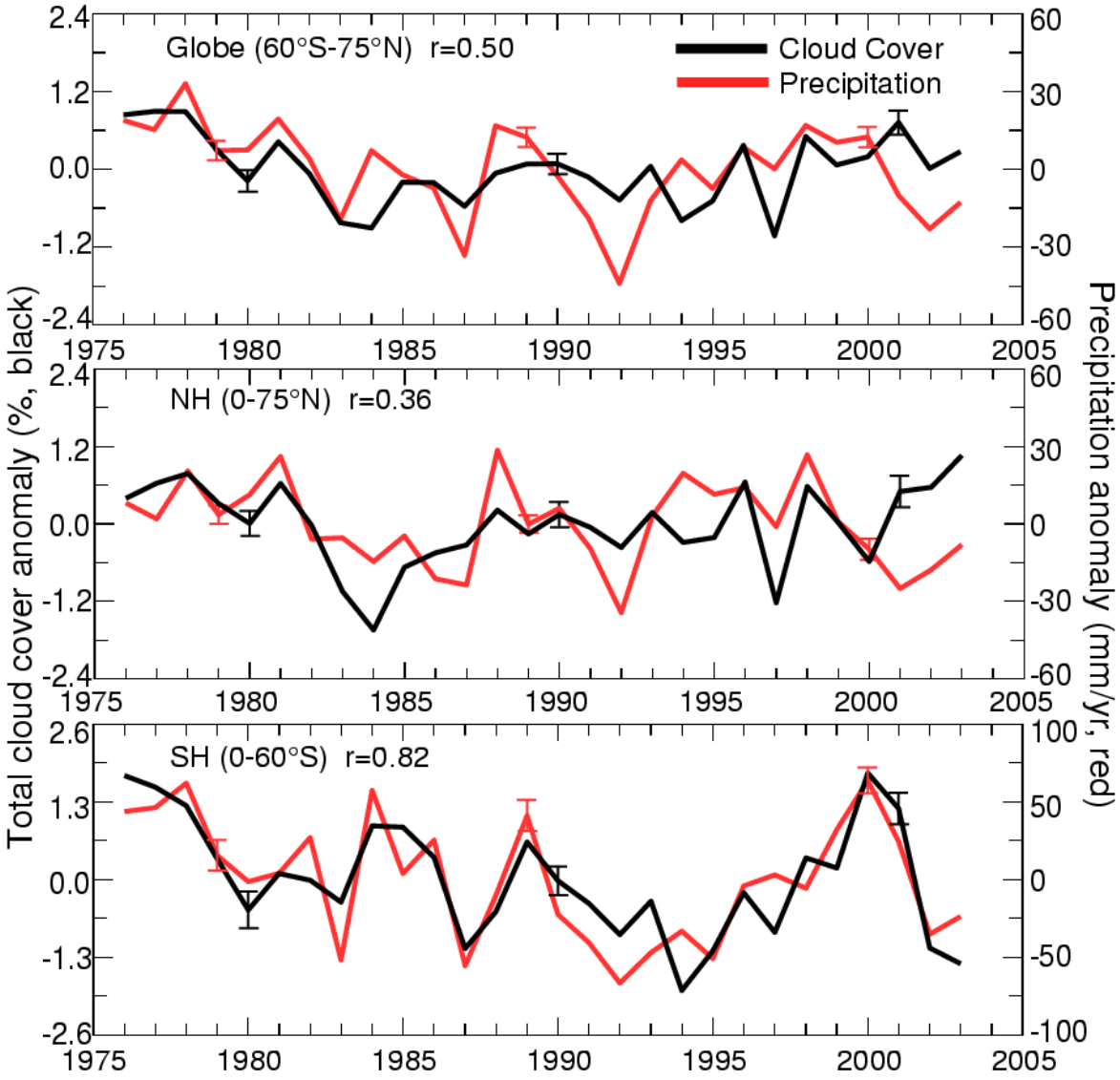

Figure 3.4.6. Annual total land (excluding the U.S. and Canada) cloud cover (black) and precipitation (red) from 1976 to 2003 over global (60°S–75°N), NH and SH regions, with the correlation coefficient (r) shown at the top. The cloud cover is derived by gridding and area-averaging synoptic observations and the precipitation is from Chen et al (2002). Error bars are one standard error estimates using inter-grid-box variations (from Dai et al., 2005).

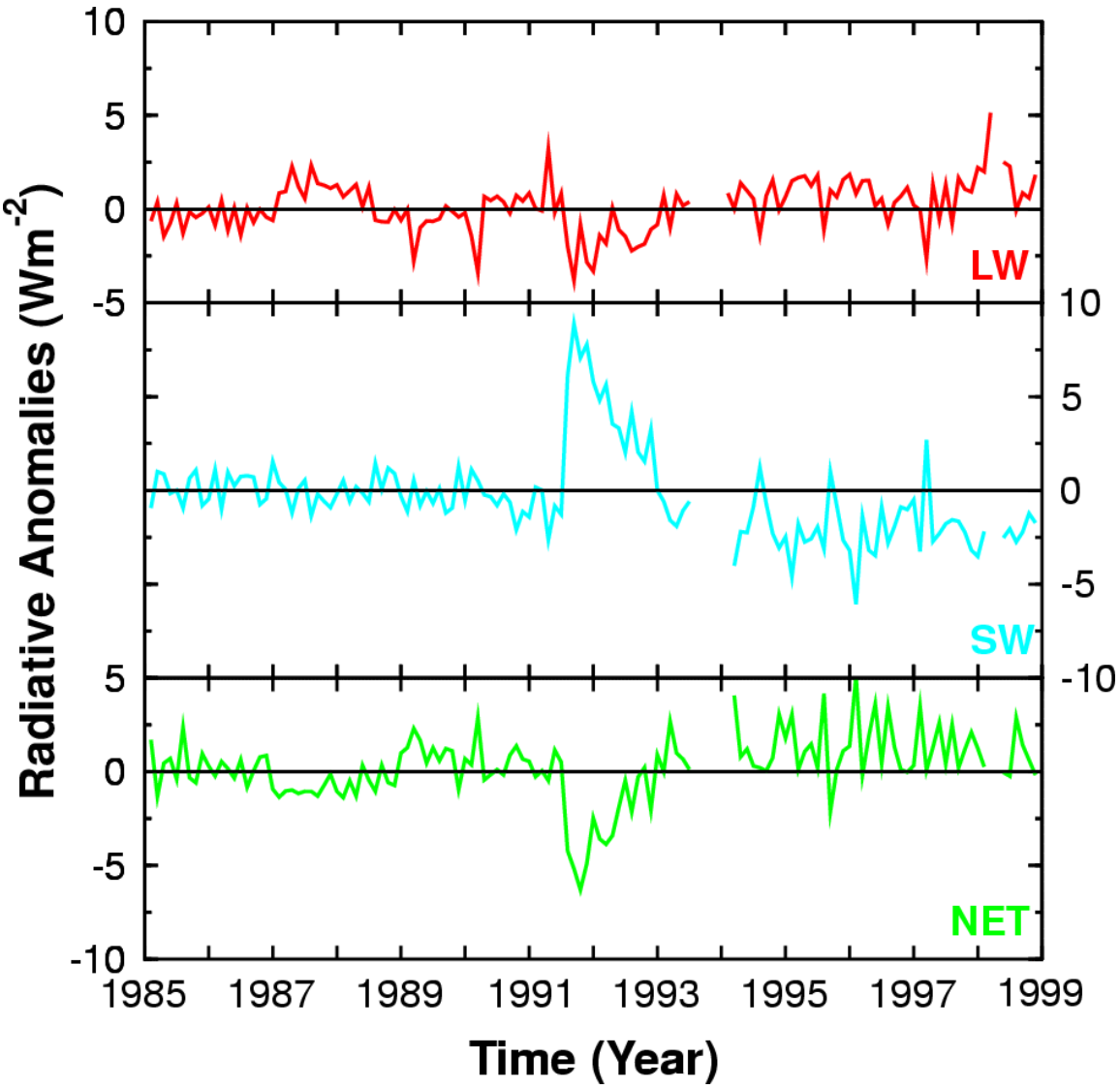

Figure 3.4.7. Tropical mean (20ºS to 20ºN) TOA flux anomalies for LW, SW, and NET radiative fluxes from 1985 to 1999. Coloured lines are observations from ERBS Edition 3_Rev1 data from Wong et al. (2005), updated from Wielicki et al. (2002a) including spacecraft altitude and SW dome transmission corrections.

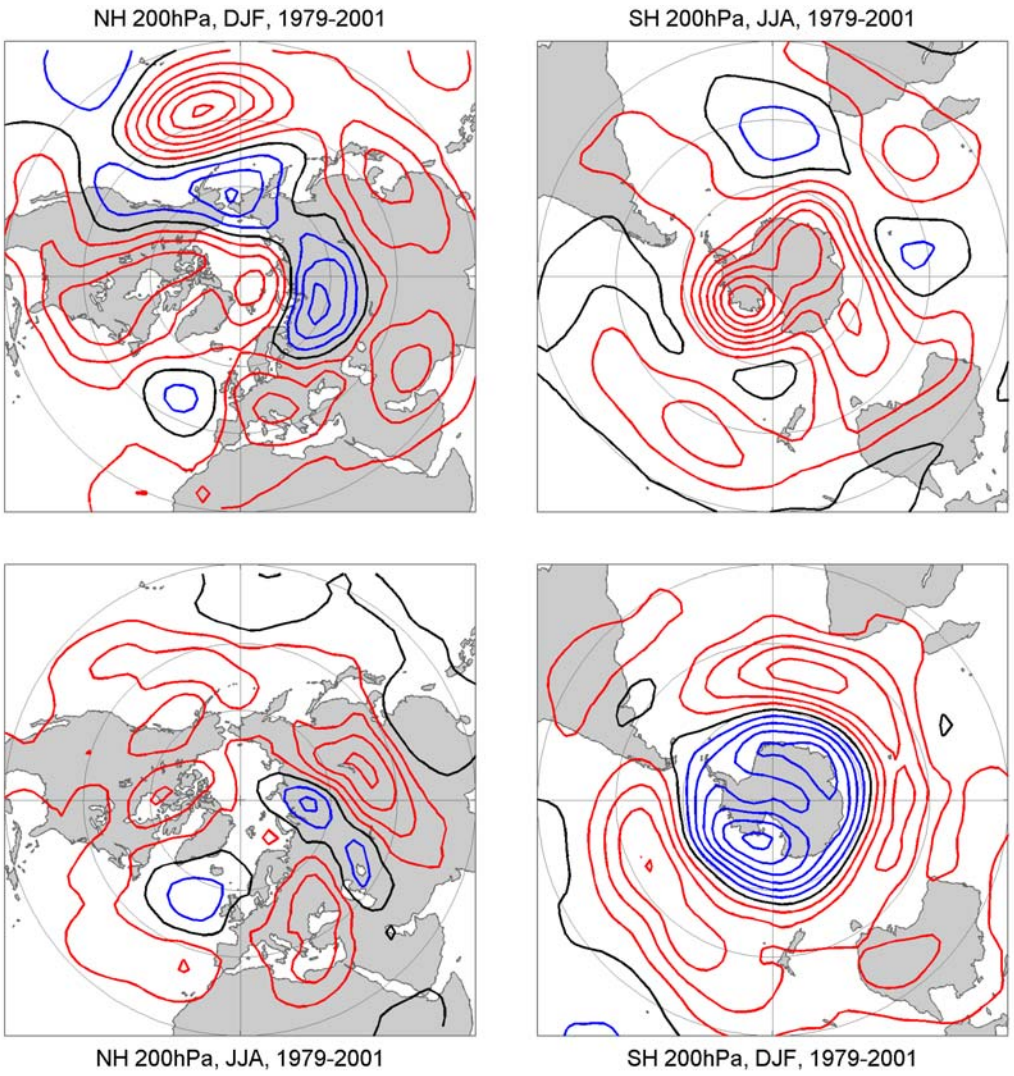

Figure 3.5.1. Height changes (in gpm) of the ERA-40 200 hPa geopotential height fields from 1979–2001 for DJF for (a) and (d) and JJA for (b) and (c), for the NH (left) and SH (right). The changes are calculated by multiplying the slope of the linear regression line at each grid point by the time interval (23 years). Averages use only 1200 UTC fields every day. Trends calculated linearly from seasonal means. Contour interval 20m, red contours positive, blue negative, and black zero. Adapted from Bromwich and Fogt (2005).

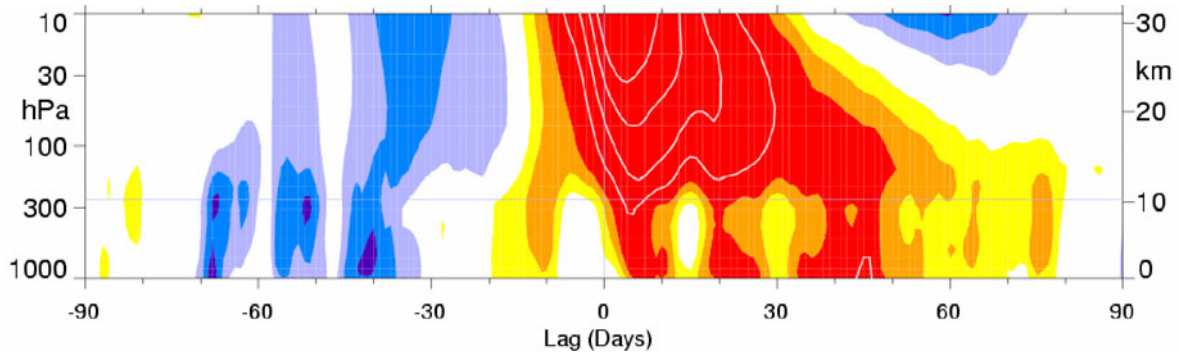

Box 3.2, Figure 3.5.2. Composites of time-height development of the northern annular modes for 18 weak vortex events. The events are determined by the dates on which the 10 hPa annular mode values cross –3.0. The indices are nondimensional; the contour interval for the colour shading is 0.25, and 0.5 for the white contours. Values between –0.25 and 0.25 are unshaded. The thin horizontal lines indicate the approximate boundary between the troposphere and the stratosphere. Modified from Baldwin and Dunkerton (2001).